Cerebral Cortex October 2009;19:2308–2320
doi:10.1093/cercor/bhn247
Advance Access publication February 4, 2009

Input Specificity and Dependence of Spike Timing–Dependent Plasticity on Preceding Postsynaptic Activity at Unitary Connections between Neocortical Layer 2/3 Pyramidal Cells

Misha Zilberter[1,2], Carl Holmgren[3,4], Isaac Shemer[1], Gilad Silberberg[1], Sten Grillner[1], Tibor Harkany[2,5] and Yuri Zilberter[1,4]

[1]Department of Neuroscience, Karolinska Institutet, SE-17177 Stockholm, Sweden, [2]Division of Molecular Neurobiology, Department of Medical Biochemistry and Biophysics, Karolinska Institutet, SE-17177 Stockholm, Sweden, [3]Department of Experimental Neurophysiology, CNCR, Vrije Universiteit, NL-1081HV Amsterdam, the Netherlands, [4]Institut de Neurobiologie de la Mediterranee (INMED), F-13273 Marseille Cedex 09, France and [5]Institute of Medical Sciences, College of Life Sciences and Medicine, University of Aberdeen, Aberdeen AB25 2ZD, UK

Misha Zilberter and Carl Holmgren have contributed equally to this work. Dr. Harkany and Dr. Zilberter share senior authorship.

Layer 2/3 (L2/3) pyramidal cells receive excitatory afferent input both from neighbouring pyramidal cells and from cortical and subcortical regions. The efficacy of these excitatory synaptic inputs is modulated by spike timing–dependent plasticity (STDP). Here we report that synaptic connections between L2/3 pyramidal cell pairs are located proximal to the soma, at sites overlapping those of excitatory inputs from other cortical layers. Nevertheless, STDP at L2/3 pyramidal to pyramidal cell connections showed fundamental differences from known STDP rules at these neighbouring contacts. Coincident low-frequency pre- and postsynaptic activation evoked only LTD, independent of the order of the pre- and postsynaptic cell firing. This symmetric anti-Hebbian STDP switched to a typical Hebbian learning rule if a postsynaptic action potential train occurred prior to the presynaptic stimulation. Receptor dependence of LTD and LTP induction and their pre- or postsynaptic loci also differed from those at other L2/3 pyramidal cell excitatory inputs. Overall, we demonstrate a novel means to switch between STDP rules dependent on the history of postsynaptic activity. We also highlight differences in STDP at excitatory synapses onto L2/3 pyramidal cells which allow for input specific modulation of synaptic gain.

Keywords: neocortex, pyramidal cells, synaptic plasticity

Introduction

Neocortical pyramidal cells receive and process information from a wide variety of cortical and subcortical regions. In neocortical layer 2/3 (L2/3), information processing occurs in subnetworks of adjacent pyramidal cells embedded within larger local neuronal networks (Yoshimura et al. 2005; Feldmeyer et al. 2006). Consequently, it is important to determine how temporally coordinated neuronal activity affects plasticity at synaptic connections between neighboring L2/3 pyramidal cells.

Spike timing–dependent plasticity (STDP), in which the precise timing between action potentials (APs) in pre- and postsynaptic neurons determines changes in synaptic gain, is an extensively studied form of synaptic modification due to its possible significance in vivo (Mehta et al. 1997; Lambert et al. 1998; Froemke and Dan 2002; Zhou et al. 2003). A narrow transition-window between maximal potentiation and maximal depression has been demonstrated in several STDP studies (Aizenman et al. 1998; Lambert et al. 1998; Froemke and Dan 2002; Celikel et al. 2004; Tzounopoulos et al. 2004). This striking switch between the induction of synaptic potentiation or depression provides the basis for spike-based, temporally asymmetric Hebbian learning rules (Bi and Poo 2001; Roberts and Bell 2002; Rubin et al. 2005).

Following the definition by Roberts and Bell (2002), the term ''Hebbian'' is used here to describe synaptic plasticity in which potentiation of an excitatory postsynaptic potential [EPSP] occurs if a presynaptic spike is accompanied by an increase in the probability of a postsynaptic spike during the period of association, and the term ''anti-Hebbian'' is used to describe synaptic plasticity in which depression of the EPSP occurs under such conditions. The term ''symmetric'' refers to the phenomenon when the direction of the change in the synaptic gain is the same independent of the pairing order (pre–post vs. post–pre). Consequently, ''asymmetric'' represents plasticity where depression switches into potentiation if the pairing order is reversed.

However, asymmetric anti-Hebbian STDP has been observed in the dorsal cochlear nucleus of the brainstem (Tzounopoulos et al. 2004; Tzounopoulos et al. 2007), whereas symmetric anti-Hebbian learning rules operate at intralaminar L4 spiny stellate cell (Egger et al. 1999) and L2/3 to L5 pyramidal cell unitary connections (Letzkus et al., 2006; Sjöström and Häusser 2006), indicating the cellular specificity and spatial diversity of STDP rules in different brain structures.

In studies of STDP, backpropagating APs (bAPs) provide the crucial associative link between synaptic activation, elevation of postsynaptic dendritic spine Ca^{2+} concentration ($[Ca^{2+}]_{post}$), and synaptic plasticity (Magee and Johnston 1997; Markram et al. 1997; Bi and Poo 1998; Debanne et al. 1998; Köster and Sakmann 1998; Feldman 2000; Sjöström et al. 2001, 2003; Froemke and Dan 2002; Celikel et al. 2004; Tzounopoulos et al. 2004; Sjöström and Häusser 2006). A key function of bAPs in this process is the depolarization-induced relief of *N*-methyl-D-aspartate receptor (NMDAR) channels from Mg^{2+} block and subsequent increase in synaptic Ca^{2+} influx. However, attenuation of the bAP as it travels into the dendrites means that its ability to modulate synaptic strength at distal synapses may be reduced both in slices and in vivo; and other forms of synaptic plasticity based on dendritic spikes may operate at these sites (Goldberg et al. 2002; Golding et al. 2002; Mehta 2004; Lisman and Spruston 2005; Gordon et al. 2006; Kampa et al. 2006). This phenomenon has been suggested to be a mechanism for input

specificity in cortical pyramidal cells. Additionally, activation of particular signaling pathways including those downstream from metabotropic glutamate receptors (mGluRs) (Bender et al. 2006; Nevian and Sakmann 2006) and CB_1 cannabinoid receptors (CB_1R) (Sjöström et al. 2003; Tzounopoulos et al. 2007) can contribute to STDP induction, resulting in input-specific STDP rules (for review, see Kampa et al. 2007).

We studied STDP induction at unitary synaptic connections between neocortical L2/3 pyramidal cells. We show that although synaptic contacts at these connections appear proximal to the soma, pairing single EPSPs with single postsynaptic bAPs induces LTD irrespective whether the presynaptic activation precedes or follows the postsynaptic activation, resulting in a symmetric, anti-Hebbian learning rule at these synapses. Additional postsynaptic depolarization or even complete relief of the NMDAR Mg^{2+} block does not change the outcome of this standard spike-pairing protocol, suggesting that the failure to induce LTP is not location-dependent, as previously suggested for excitatory inputs onto L5 and L2/3 pyramidal cells. However, if single presynaptic EPSPs are preceded by a train of 8 or more bAPs (at 50 Hz), the plasticity rule switches to a typical Hebbian timing dependence for both LTP and LTD. This switch relies on the elevation of the $[Ca^{2+}]_{post}$ prior to synaptic activation, predominantly via L-type voltage-gated Ca^{2+} channels (VGCCs). Thus, in L2/3 pyramidal cell pairs, the postsynaptic activity occurring shortly before the synaptic input can determine which synaptic plasticity rule will govern the strength of the unitary connection. In addition, we report that the requirement for STDP rules in L2/3 pyramidal-to-pyramidal (P–P) connections is accompanied by synaptic properties that differ from those reported previously for other excitatory inputs onto cortical pyramidal cells. Namely, we show that at these connections LTP is presynaptic, CB_1R independent, mGluR independent but NMDAR dependent; whereas LTD is CB_1R independent, NMDAR independent but mGluR dependent. Altogether, our data suggest that single L2/3 pyramidal cells are able to distinguish between different presynaptic sources even when input locations overlap, and form physiologically distinct synapses accordingly.

Materials and Methods

Electrophysiology

Parasagittal cortical slices (300 μm) were prepared from 14- to 21-day-old Sprague–Dawley rat pups, with slice orientation chosen to minimize axonal cutting (Holmgren et al. 2003). Extracellular solution contained (in mM): 125 NaCl, 2.5 KCl, 2 $CaCl_2$, 1 $MgCl_2$, 25 $NaHCO_3$, 1.25 NaH_2PO_4, and 25 glucose. Pipette solution contained (in mM): 135 K-gluconate, 20 KCl, 4 ATP-Mg, 10 Na-phosphocreatine, 0.3 GTP, and 10 4-(2-hydroxyethyl)-1-piperazineethanesulfonic acid, pH 7.3 (with 100 μM fura-2 (Molecular Probes, Leiden, The Netherlands) in fluorescence imaging experiments; fura-2 was not included in any experiments where STDP has been recorded). All experiments were performed at 32–34 °C. In cases where antagonists or agonists were applied, drugs were present in the solution throughout the experiment.

Pyramidal cells located in L2/3 of the visual cortex, identified using infrared differential interference contrast microscopy, were selected on the basis of morphology and the subsequent characterization of their firing patterns. ΩOhm seals were obtained on 2 or 3 pyramidal cells typically within 25 μm from each other. Recordings were performed on independent pyramidal cell pairs or triplets. If no connection was found a new pair or triplet was used instead. Connectivity was assessed by averaging 10–15 traces and connections with low release probability were discarded. In Mg^{2+}-free experiments, slices were superfused with nominally Mg^{2+}-free external solution for at least 20 min prior to initiating the experiment to achieve stability without hyperactivity in the slice.

Recordings were made using Axopatch 200B and Axoclamp 2B amplifiers (Axon Instruments, Foster City, CA), sampled at 50- or 100-μs intervals, digitized by an ITC-18 interface (Instrutech, Port Washington, NY) and analyzed off-line (Igor Wavemetrics, Lake Oswego, OR). Borosilicate glass patch pipettes had a resistance of 3–5 MΩ. Series resistance was not compensated. Cell input resistance (average = 157 ± 11 MΩ) was monitored throughout the experiments by applying a 11 pA, 300-ms hyperpolarizing pulse at the end of each sweep. Experiments were excluded if the resting membrane potential deviated by more than 5 mV, input resistance deviated by more than 30%, or if baseline recording changed significantly (Supplementary Fig. 1). In each experiment, mean EPSPs measured in control were averaged from at least 50 sweeps (7-s intersweep intervals). During conditioning protocols for induction of plasticity, pre- and postsynaptic pyramidal cells were stimulated 40 times, every 5 s. Postinduction measurements were started immediately after completion of the conditioning protocol. Synaptic change was estimated for the period 5 min after the conditioning until the end of the experiment.

Paired-pulse ratios (PPRs) were calculated as EPSP2/EPSP1, where EPSP1 and EPSP2 were the average postsynaptic potential amplitudes in response to the first and second APs in a presynaptic cell (100-ms interpulse interval).

In experiments where the single pre- and postsynaptic AP protocol was combined with an additional EPSP evoked by extracellular stimulation (0.2-ms pulse duration, 7–8 mV), the stimulating electrode was placed in lower L1 (L2/3 experiments) or lower L4 (L5 experiments). For experiments with VGCC blockade by the intracellular L-type channel antagonist methoxyverapamil (D890), connected cell pairs were first identified using pipettes with normal intracellular solution. The postsynaptic cell was then repatched with a pipette containing 200 μM D890. Fifteen minutes were allowed for drug diffusion before the start of the baseline recordings.

During experiments in which the calcium chelator 1,2-bis(*o*-aminophenoxy) ethane-*N*,*N*,*N*′,*N*′-tetraacetic acid (BAPTA, Sigma) was introduced postsynaptically via the patch pipette, at least 5 min were allowed for buffer diffusion. This period corresponds to a mean-squared displacement of 270 μm (calculated for a cytoplasmic diffusion coefficient of 200 $\mu m^2/s$ described by Naraghi and Neher 1997), which is 7.5 times the average distance from the soma to L2/3 pyramidal cell synaptic contacts (36.5 ± 5.4 μm).

Induction of LTP Using Extracellular Stimulation

Baseline, conditioning and postconditioning durations, stimulus frequencies and conditions were as described above for unitary L2/3 P–P cell connections. EPSPs were evoked using an extracellular stimulation electrode positioned in L2/3 at a distance of 50–100 μm lateral to the recorded pyramidal cell. Initial EPSP amplitudes were between 1 and 3 mV. The initial EPSP slope was measured to ensure that data reflected monosynaptic input in each experiment. Cl^- concentration in the intracellular solution was adjusted so that the calculated Cl^- reversal potential was close to the resting membrane potential. No significant difference was observed in the degree of LTP induction in the presence (1.33 ± 0.15; $n = 5$), or absence (1.34 ± 0.12; $n = 10$; $p > 0.5$) of gabazine (1 μM; Sigma), γ-aminobutyric acid receptor A ($GABA_AR$) antagonist that does not affect GABA-transaminase or glutamate-decarboxylase activities, and data were consequently pooled. During the induction protocol spike timings were measured from the onset of the evoked EPSP to the peak of the postsynaptic AP.

Morphometric Analysis of Pyramidal Cell Connections

Pre- and postsynaptic neurons in connected pyramidal cell pairs were intracellularly labeled with biocytin (0.5 mg/mL; Sigma) and Alexa Fluor 488 (0.5–1.0 mM; Molecular Probes), respectively. The presynaptic neuron was always filled with biocytin for at least 20 min, as this gave the strongest signal when fluorochromated streptavidin (Jackson ImmunoResearch, West Grove, PA) was used and allowed ready identification and visualization of presynaptic boutons. Brain slices

were fixed by immersion in 4% paraformaldehyde and 0.1% glutaraldehyde in phosphate buffer (PB, 0.1 M, pH 7.4) overnight. Following repeat washes in PB, slices were preincubated in PB containing 1% Triton X-100 in PB for 1 h. The tissue was then extensively rinsed in PB and the cellular distribution of biocytin was revealed by carbocyanine (Cy)3-tagged streptavidin (0.25 μg/mL; Jackson) in 2% bovine serum albumin (BSA) and 0.5% Triton X-100 in PB overnight at 4 °C.

Analysis of our specimens was performed using a confocal laser-scanning microscope (Model 510, Zeiss, Jena, Germany) equipped with argon (488 nm) and helium-neon (543 nm) lasers and appropriate excitation and emission filters for maximum separation of Alexa Fluor 488 and Cy3 signals. Emission wavelengths were limited to 505–530 nm (bandpass filter, Alexa Fluor 488), and 560–610 nm (bandpass filter, Cy3). Identification of synapses was carried out by capturing consecutive images with an 85-μm pinhole size at 63× primary magnification (0.8 μm optical slice thickness, Fig. 1) and 1.3× optical zoom as previously described (Harkany et al. 2004). Confocal imaging was always performed shortly after the pairs were filled and the slices fixed, to avoid problems with fading or a reduction in signal of the Alexa Fluor 488 dye over time. Intersections of biocytin-filled presynaptic axons and Alexa Fluor 488–labeled postsynaptic dendritic spines were only considered as putative sites of synaptic contacts when no spatial signal separation between pre- and postsynaptic profiles in 3-dimensionally reconstructed orthogonal image stacks was evident (Fig. 1*A*,*B*). Subsequently, the distances of putative synapses from the soma were measured from images of 6 connected pyramidal cell pairs, and a map of synaptic locations was then generated (Fig. 1*C*). The locations of synaptic contacts were displayed on a generic postsynaptic pyramidal cell (Fig. 1*C*) with the distances and dendritic branch orders being preserved. Distances of putative synapses measured from the projection images are assumed to be correct, as the calculated correction factor (in the *x*–*y* plane) for postfixed and processed tissue was 1.04, based on measurements of cortical thickness pre- and postfixation/processing (n = 20 slices from 2 rats). Images were processed and off-line analyzed by using Zeiss LSM Viewer software (v. 3.2.0.115, Zeiss, Germany). After conversion to high-resolution TIFF format, exported images were processed using CorelDraw X3 (Corel Corp., Ottawa, Canada). Data were expressed as means ± SEM. Statistical significance was determined by the paired Student's *t*-test.

Calcium Imaging

Imaging was performed using a MicroMax CCD camera (Roper Scientific, Tucson, AZ) fitted onto an upright microscope equipped with a 60× water immersion objective (BX50WI, Olympus Optical, Hamburg, Germany). During measurements, the cell was illuminated by a polychromatic illumination system (TILL Photonics, Munich, Germany). Regions of interest (ROIs) were placed on the oblique dendritic shafts 50–100 μm from the soma and the combined average Fura-2 fluorescence intensity (F) of enclosed pixels was sampled at 100 Hz. A separate ROI was placed in the neighboring region to provide background fluorescence subtraction (B). Data were then used to calculate the fluorescence ratio, R = (F356 – B356)/(F380 – B380). Traces are given as averages of 5–10 sweeps.

Results

Synaptic Contacts between L2/3 Pyramidal Cells Map onto Proximal Dendrites

To determine the precise location of synaptic contacts between neighboring L2/3 pyramidal–pyramidal cells, we mapped the locations of putative synapses between presynaptic axonal boutons and postsynaptic dendrites (Fig. 1). A putative synapse was defined by 1) a lack of spatial signal separation (≤0.2 μm) between Cy3-tagged biocytin (presynaptic label) and Alexa Fluor

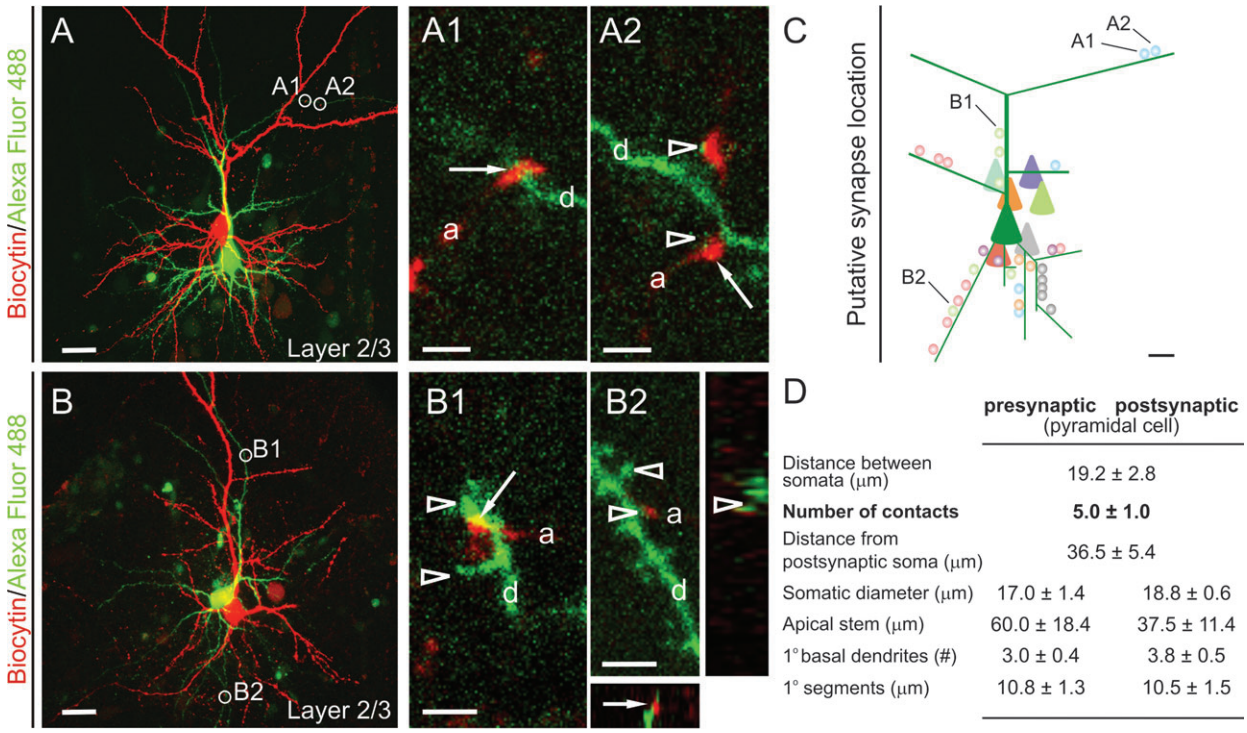

Figure 1. Layer 2/3 pyramidal-to-pyramidal cell synaptic connections. (*A*, *B*) Synaptically connected pyramidal cell pairs. Presynaptic neurons are in red (biocytin/Cy3-streptavidin), whereas postsynaptic cells appear in green (Alexa Fluor 488). Open circles denote the location of putative synaptic contacts shown in (*A1–B2*). (*A1–B1*) Image stacks of synaptic contacts were rotated to provide maximal spatial resolution between pre- and postsynaptic structures. Putative synaptic boutons (*arrows*) formed by pyramidal cell axons (*a*) target dendritic (*d*) spines (*arrowheads*) on postsynaptic pyramidal cells. Figure B2 shows orthogonal views of consecutive planar images (*z*-stack) to unequivocally identify a synaptic contact (*arrow*) on a dendritic spine (*arrowheads*) of a proximal basal dendrite segment. (*C*) Schematic map of the location of synaptic contacts, from 6 identified pyramidal cell pairs. Somatic locations of presynaptic neurons are presented by preserving their distances in slices, whereas postsynaptic neurons (green) were superimposed. Colors of postsynaptic spines correspond with the color of each presynaptic neuron. (*D*) Morphometric parameters of individual neurons used to map synapse locations in (*C*). Scale bars = 30 μm (*A*, *B*), 10 μm (*C*), 2 μm (*A1-B2*).

488 (postsynaptic marker) as defined by high-resolution laser-scanning microscopy; 2) varicose expansion of the presynaptic axon reminiscent of a synaptic bouton; 3) contact with a postsynaptic dendritic spine, the preferred site of excitatory innervation (Fig. 1*A,B*). The long time of intracellular dye application (⩾20 min) together with the above criteria prevented oversampling the number of putative synapses between synaptically connected pyramidal cell pairs. In agreement with Feldmeyer et al. (2006), connections were found primarily on proximal apical and/or basal dendrites (Fig. 1*A*–C). Overall, a postsynaptic pyramidal cell received 5 ± 1 synaptic contacts (Fig. 1*C,D*). Putative synaptic contacts on basal dendrites mapped markedly closer (25.4 ± 2.7 μm; n = 21) to neuronal somata than apical contacts (62.5 ± 13.6 μm; n = 9) (Fig. 1*C,D*). Although L2/3 pyramidal cells displayed a variety of apical tuft morphologies (Fig. 1*A,B*), the number, intralaminar distribution, and lengths of their basal dendrites appeared largely uniform (Fig. 1*D*). Given that the location of identified synaptic contacts arising from neighboring pyramidal cells mapped onto proximal dendrites, it is likely that bAPs reliably reach active synapses both in acute brain slice preparations (Köster and Sakmann 1998) and in vivo (Svoboda et al. 1999; Waters et al. 2003).

Single EPSP-Postsynaptic bAP Protocols Induce LTD at Synapses between L2/3 Pyramidal Cells

A simple asymmetric Hebbian learning rule has been shown to regulate synaptic plasticity at excitatory synapses onto L2/3 pyramidal cells (Feldman 2000; Froemke and Dan 2002; Froemke et al. 2005): pairing a single extracellularly evoked EPSP with a single postsynaptic bAP induces LTP if the EPSP precedes the bAP by a short (ms) time interval (Figs 2A and 3; synaptic gain: 1.34 ± 0.09, n = 15; P < 0.01).

Using this simple pre-before-post pairing protocol we tested whether a similar rule governs synaptic plasticity specifically at unitary L2/3 P–P synaptic connections. However, following the same single pre-before-postsynaptic AP pairing protocol in synaptically connected L2/3 pyramidal cell pairs (Δt = 10 ms), LTD and not LTP was induced (synaptic gain: 0.64 ± 0.07; n = 6, P < 0.05; see Figs 2*B* and 3). To ensure that this observation was not just the consequence of an even narrower coincidence detection window for LTP induction at these unitary connections, we reduced the time interval between the pre- and postsynaptic APs (Δt within 2–5 ms), which resulted in a similar LTD outcome (synaptic gain: 0.77 ± 0.09 of control; n = 5, P < 0.05; data not shown). To confirm that the changes in synaptic plasticity were not the result of rundown during the recording period or instability in the experimental set-up, we stimulated the presynaptic cell alone, at the same frequency as during the pairing protocol. The lack of change in synaptic gain (0.98 ± 0.08 of control, n = 5; Supplementary Fig. 1*B*) excluded the possibility that the changes observed were due to the above methodological artifacts.

An important role of the bAP in STDP induction is the relief of NMDARs from Mg^{2+} block. This can be facilitated by a depolarization of the postsynaptic cell, or by using Mg^{2+} free extracellular solution. Neither somatic subthreshold depolarization (to –45.5 ± 1.77 mV), nor synaptically induced depolarization (concurrent extracellularly evoked EPSP; 8.3 ± 0.65 mV) during the single pre- and postsynaptic AP pairing period induced LTP (synaptic gain with somatic depolarization: 0.84 ± 0.05 of control; n = 8, P < 0.05; Figs 2*C* and 3; synaptic gain with concurrent extracellularly evoked EPSP: 0.82 ± 0.06 of control, n = 5, P < 0.05; Figs 2*D* and 3; Supplementary Fig. 2). Importantly, under the same experimental conditions, the latter stimulation protocol effectively induced LTP at L5 P–P synaptic connections (in agreement with Sjöström et al. 2001) (1.34 ± 0.01 of control, n = 5, P < 0.05, with a 7.2 ± 0.6 mV concurrent extracellularly evoked EPSP, Figs 2*E* and 3; Supplementary Fig. 2).

We subsequently tested the single pre- and postsynaptic AP protocol (Δt = 10 ms) in Mg^{2+}-free extracellular solution, effectively removing NMDAR's voltage dependence, which still resulted in the induction of LTD (0.72 ± 0.07 of control; n = 5, P < 0.02; Figs 2*F* and 3).

Thus, none of the standard single EPSP-postsynaptic bAP stimulation protocols induce LTP at L2/3 P–P unitary connections, but instead induce LTD, even when 1) Δt is decreased to 2–5 ms, 2) coupled with additional postsynaptic depolarization, or 3) in the absence of extracellular Mg^{2+}. 4) LTD is also induced when the order in which single post- and presynaptic APs occurs is reversed (post–pre pairing, Δt = –10 ms; synaptic gain: 0.56 ± 0.06 of control, n = 4, P < 0.01; data not shown). Therefore, a symmetric anti-Hebbian rule governs synaptic plasticity at L2/3 P–P synapses when single EPSPs are paired with single postsynaptic APs.

Pairing Low-Frequency Pre- and Postsynaptic AP Bursts

At L5 P–P synaptic connections, an increase in the number of coincident pre- and postsynaptic APs, using trains of 5 pre- and 5 postsynaptic APs, allows for reliable induction of LTP even with low-frequency (10 Hz) stimulation (Markram et al. 1997; Sjöström et al. 2001). At L2/3 P–P synaptic connections, LTD was induced with this protocol (0.76 ± 0.07 of control; n = 19, p < 0.01; Figs 2*G* and 3). However, an increase in the train frequency to 20 Hz (pre–post) shifted the gain towards LTP, abolishing LTD induction (1.07 ± 0.11 of control, n = 6, Fig. 2*H*, Fig. 3). Additionally, with a 5–5 post–pre AP protocol at 20 Hz (postsynaptic APs occurring 10 ms prior to the presynaptic APs) LTD was not induced (0.93 ± 0.07; n = 5, data not shown).

Postsynaptic AP Train Permits LTP Induction and Changes the Synaptic Learning Rule

Further increases in the frequency of the 5–5 pre–post AP trains should increase synaptic gain and induce LTP (Markram et al. 1997; Egger et al. 1999; Sjöström et al. 2001) at L2/3 P–P synaptic connections. However, with this stimulation protocol there are multiple spike-timings as 5 presynaptic activations are interacting with 5 postsynaptic APs, producing multiple Δt values. Additionally, short-term synaptic plasticity affects the contribution of each presynaptic AP to the synaptic plasticity outcome. Presynaptic failures can occur at any time during the train, thus coinciding with different postsynaptic APs and resulting in different and unpredictable postsynaptic Ca^{2+} levels. These nonlinear interactions complicate the process of dissecting out the contribution of any one presynaptic AP to the resultant change in synaptic plasticity.

We therefore modified our stimulation protocol. In particular, we tested the effect of the pattern of activity in the postsynaptic neuron prior to synaptic activation on both the change in synaptic gain and the simple STDP rule. The postsynaptic firing pattern was changed to a train of APs (10 APs at 50 Hz; Fig. 4) to evoke dendritic Ca^{2+} influx through

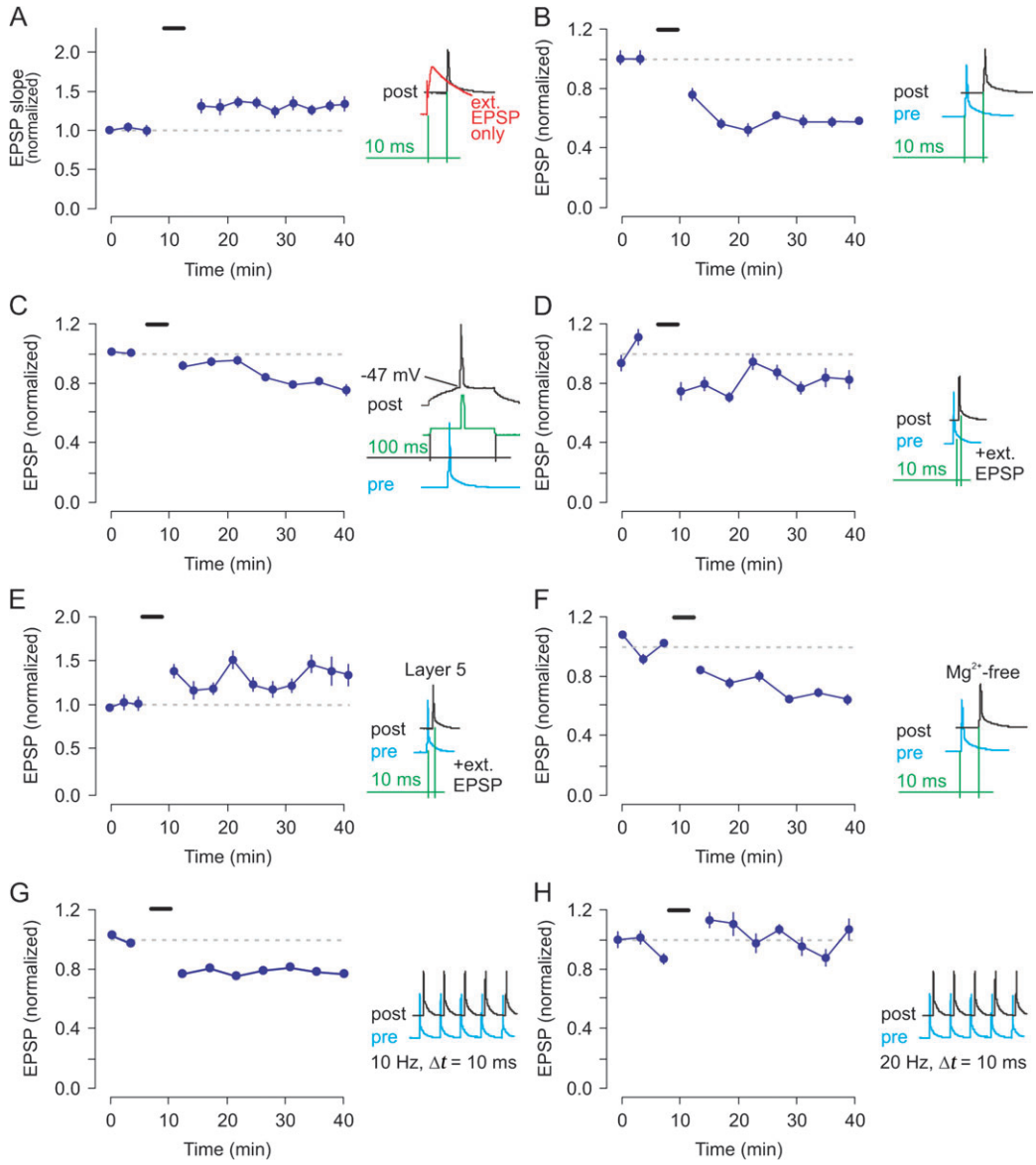

Figure 2. LTD induced by pre-before-postsynaptic stimulation at synapses between L2/3 pyramidal cells. (*A*) Pre–post pairing (Δt = 10 ms); extracellularly induced EPSP paired with a single postsynaptic AP. (*B*) Stimulation with single pre- and postsynaptic APs (pre–post pairing). (*C*) Pre–post pairing (Δt = 10 ms) with additional subthreshold postsynaptic depolarization. (*D*) Pre–post pairing (Δt = 10 ms); unitary EPSP coincident with a large extracellularly induced EPSP. (*E*) Pre–post pairing (Δt = 10 ms); unitary EPSP coincident with a large extracellularly induced EPSP in pairs of connected L5 pyramidal neurons. Extracellularly induced EPSP was elicited during the induction period only and not for baseline or postinduction measurements in both D and E. (*F*) Single pre- and postsynaptic APs (pre–post pairing) in the absence of Mg^{2+}. (*G*) Stimulation with trains of 5 pre- and 5 postsynaptic APs at 10 Hz. (*H*) Stimulation with trains of 5 pre- and 5 postsynaptic APs at 20 Hz. The graphs show the average of experiments (n = 15 for (*A*), n = 10 for (B); n = 8 for (*C*), n = 5 for (*D*), n = 5 for (*E*), n = 5 for (*F*), n = 19 for (*G*), and n = 6 for (*H*)). Each data point represents mean ± SEM values binned over a period of 3 min. Graphs of corresponding sample experiments for each of the protocols introduced here can be found in Supplementary Figure 2.

VGCCs and lead to Ca^{2+} accumulation in dendrites. However, in order to observe the effects of the timing of presynaptic activation on synaptic gain we retained the single presynaptic AP.

If a single presynaptic AP was evoked 3–5 ms prior to the 10th AP in the 10 AP train, synaptic potentiation occurred in all cases (summed average of synaptic gain: 1.49 ± 0.12; n = 11, P < 0.01; Fig. 4*A*,*D*). However, if the order was reversed such that the presynaptic stimulation preceded the postsynaptic AP train, LTP was not induced (single presynaptic AP evoked 5 ms prior to the first AP in the bAP train; synaptic gain: 0.97 ± 0.06 of control, n = 4, P > 0.5; Fig. 4*B*). Additionally, the postsynaptic train alone (no presynaptic activation) was insufficient to induce LTP (1.03 ± 0.04 of control, n = 4, Supplementary Fig. 1*C*). Therefore, at L2/3 unitary P–P synaptic connections, single presynaptic stimuli can induce LTP, provided they are preceded by a postsynaptic bAP train.

To test whether a spike timing rule still operates when a postsynaptic bAP train precedes the presynaptic stimulation we evoked a single presynaptic AP after the 10th AP in the train (Fig. 4*C*,*D*), effectively making it a post–pre protocol. With a 3- to 5-ms time interval between the 10th AP and the presynaptic AP there was no significant change in synaptic gain (0.99 ± 0.09 of control, n = 6, P > 0.5; Fig. 4*D*). However, if the interval between the 10th AP in the train and the presynaptic AP was 5–12 ms, depression was reliably induced (summed average, 0.72 ± 0.05 of control, n = 13, P < 0.01; Fig. 4*C*,*D*).

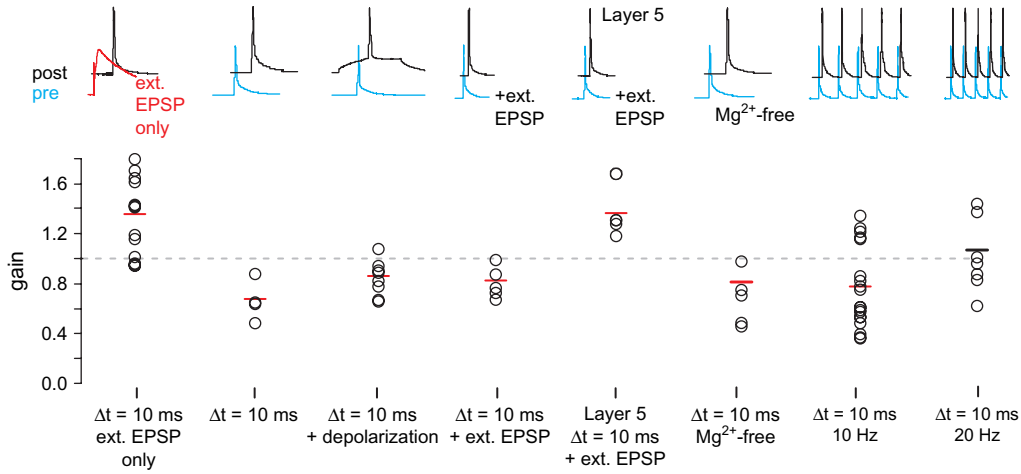

Figure 3. Effect of different stimulation paradigms on STDP induction at L2/3 P–P connections. Each open circle shows the change in synaptic gain in an individual experiment following the conditioning protocol shown above each group. Mean change in synaptic gain within each group is indicated by a horizontal bar. Significance in change from 1 (1 being no change) is represented in red bars, and black bar denotes absence of significant change.

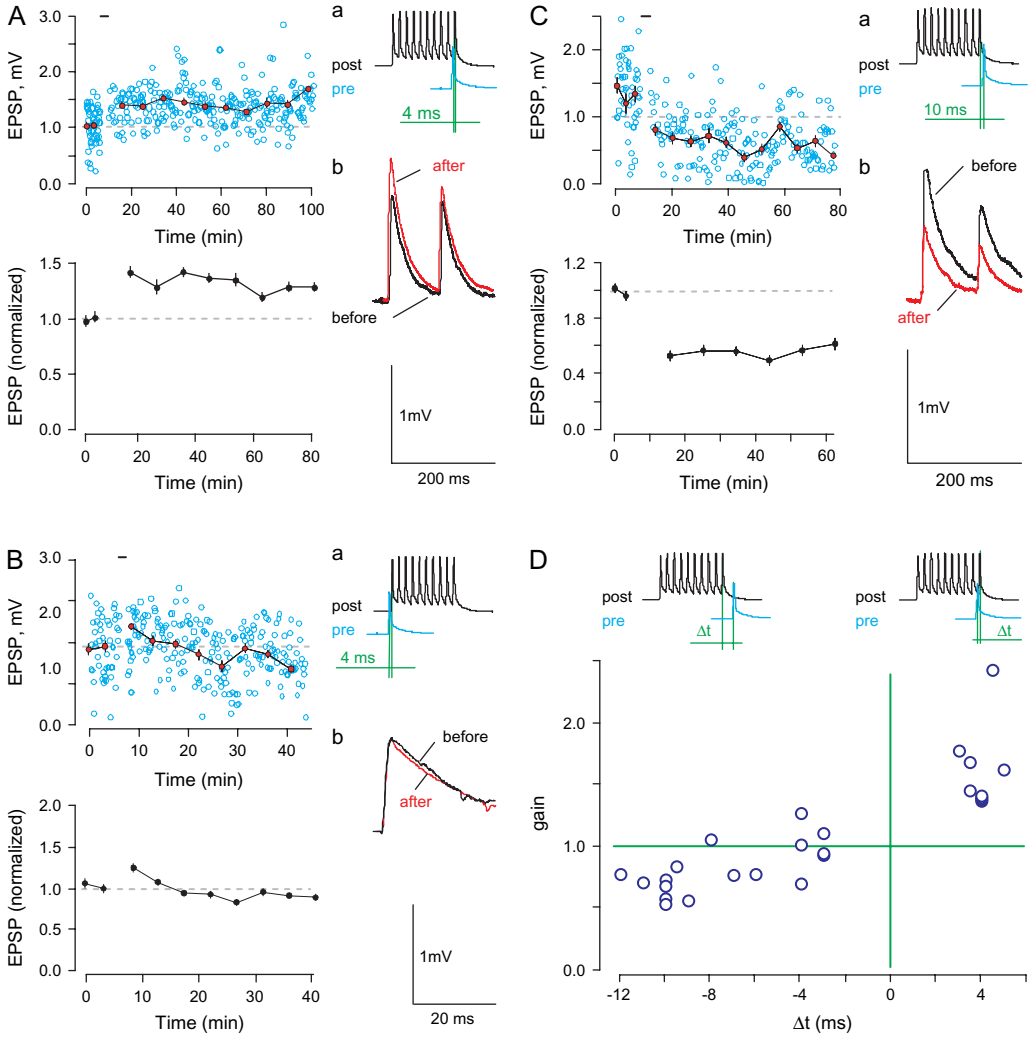

Figure 4. A postsynaptic train of bAPs rescues synaptic potentiation and establishes Hebbian plasticity at pyramidal-to-pyramidal cell synapses. (*A*) Reliable synaptic potentiation with a preceding train of bAPs (train-LTP protocol; 10 APs, 50 Hz). (*B*) No significant change in gain with "postconditioning" with an AP train. Insets (a) schematic representations of stimulation paradigms; (b) mean EPSPs pre- and poststimulation. Bottom graphs; average of experiments (n 5 6 for (A), n 5 7 for (B), n 5 4 for (C)). Each data point represents mean ± SEM data averaged within a period of 3 min. (*C*) Synaptic depression with the train-LTD protocol. (*D*) Summary of train-LTP and -LTD protocols, showing an asymmetric Hebbian rule.

In addition, we investigated the effect of both preceding-train induction paradigms in the absence of extracellular Mg^{2+}. In Mg^{2+}-free solution, both pre–post and post–pre pairing protocols with a preceding bAP train resulted in LTP induction (synaptic gain ranging from 2.0 to 5.0 of control, $n = 3$ and 1.39 ± 0.13 of control, $n = 6$, $P < 0.01$, respectively; data not shown), indicating a switch between an asymmetric Hebbian to a symmetric Hebbian rule. This highlights the importance of Ca^{2+} kinetics following synaptic activation and indicates that the failure to induce LTP with a single pre–post pairing in absence of Mg^{2+} is not due to saturation of LTP under such conditions.

At unitary connections between L2/3 pyramidal cells, a burst of postsynaptic bAPs shortly preceding synaptic activation can therefore switch the STDP rule from a symmetric anti-Hebbian to an asymmetric Hebbian one. Without the burst, coincidence of single pre- and postsynaptic APs induces LTD, independent of the order in which pre- and postsynaptic stimulation occurs. Meanwhile, following the burst, stimulation with pre–post and post–pre pairing protocols can induce both LTP and LTD, respectively.

Further in the text, stimulation protocols utilizing preceding postsynaptic AP trains are referred to as train-LTP or train-LTD.

Ca^{2+} Provided by VGCC Controls the Induction of LTP

To study the role of VGCCs in the induction of LTP we used D890, a permanently charged and membrane impermeant verapamil analogue that predominantly inhibits L-type VGCCs (200 μM), which has the advantage that it can be applied via the patch pipette to the postsynaptic cell alone. When applying D890, the amplitude of dendritic Ca^{2+} transients during the 10 AP train was reduced to 0.37 ± 0.04 of control ($n = 4$, Fig. 5*A*).

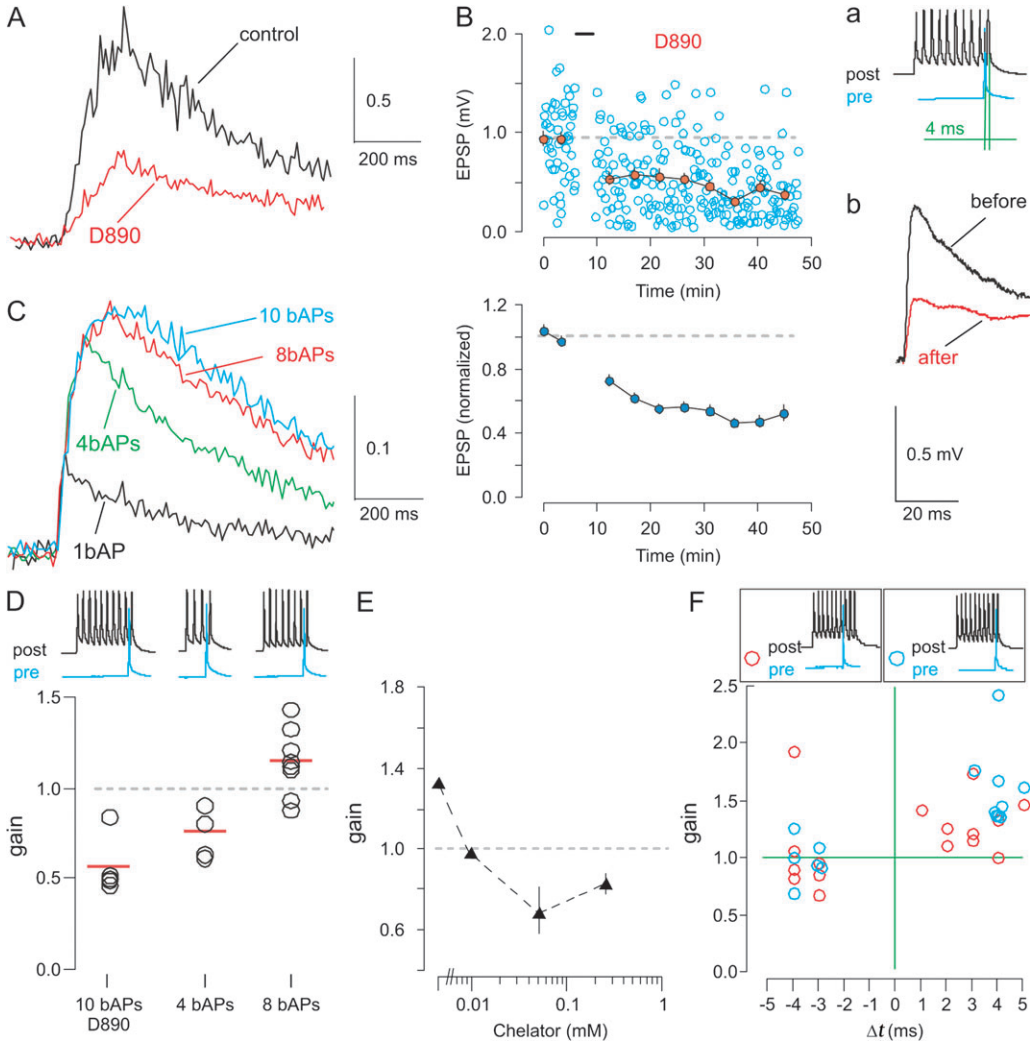

Figure 5. Regulation of basal Ca^{2+} levels by VGCCs controls LTP induction. (*A*) Dendritic Ca^{2+} transients in response to a 10 AP train (50 Hz) measured in oblique dendrites in control and after repatching with 200 μM D890. (*B*) Blockade of VGCC by 200 μM D890 prevents the induction of LTP by the train-LTP protocol, resulting in LTD instead; (*a*) schematic of the stimulation paradigm; (*b*) mean EPSPs pre- and poststimulation. Lower graph; average of 5 experiments. Each data point represents data averaged within 3 min. (*C*) Dendritic Ca^{2+} transients in response to AP trains consisting of 1, 4, 8, and 10 APs. (*D*) Summary of experiments; effect of varying dendritic basal Ca^{2+} levels on STDP. Each data point represents an individual experiment ($\Delta t = 4$ ms in all experiments). (*E*) Effect of different postsynaptic BAPTA concentrations on STDP, using a train-LTP induction protocol. Note that zero postsynaptic BAPTA point comes from Figure 4*A*. Each point shows the average change in synaptic gain from 3 to 11 experiments. Error bars show SEM. (*F*) Summary of different train-LTP protocol outcomes. Blue circles represent individual experiments with the use of standard train-LTP or train-LTD protocols, with the presynaptic activation occurring around the 10th AP in the 50 Hz train. Red circles represent individual experiments with the use of a modified stimulation protocol with a presynaptic AP shifted to the vicinity of eighth AP in the train (see inset).

As a result, the train-LTP stimulation protocol induced prominent LTD (Fig. 5*B*), which was 0.57 ± 0.07 of control ($n = 5$, $\Delta t = 4$ ms, $P < 0.01$). Meanwhile, in control experiments (without D890) a prolonged waiting period after patching but prior to conditioning did not prevent LTP induction (1.34 ± 0.11; $n = 5$, $P < 0.05$, Supplementary Fig. 1*A*). Therefore, the failure to induce LTP in the presence of D890 was not due to washout of key signaling molecules during the loading protocol. Although D890 has been shown to inhibit CaMKII, a molecule important for LTP induction, the concentration we used in this study was less than that required for 20% inhibition of CaMKII in vitro, and the actual concentration at the dendritic spine is likely to be significantly lower than this (Conti and Lisman 2002). Thus, the effect of D890 on LTP induction in our study is not likely to be due to inhibition of CaMKII activity.

As an alternative means of changing $[Ca^{2+}]_{post}$ in proximal dendrites we varied the number of postsynaptic APs in the train-LTP protocol. Figure 5*C* shows the dendritic Ca^{2+} transients corresponding to trains of 1, 4, 8, and 10 APs. Although affected by the presence of the exogenous buffer (100 μM fura-2), these transients reflect the relative change in dendritic $[Ca^{2+}]_{post}$ with the change in bAP number. Figure 5*D* shows that a train-LTP protocol consisting of only 4 APs still results in LTD (0.76 ± 0.07 of control, $n = 4$, $\Delta t = 4$ ms, $P < 0.05$). Increasing the number of bAPs to 8, however, already induces LTP (1.15 ± 0.08 of control, $n = 8$, $\Delta t = 4$ ms, $P < 0.05$). LTP induction was blocked by addition of the Ca^{2+} chelator BAPTA (0.01 mM) to the postsynaptic recording pipette (train-LTP conditioning protocol; Fig. 5*E*). Using the same train-LTP protocol but with a higher concentration of BAPTA (0.05 mM) LTD was induced. With 0.25 mM BAPTA, this LTD induction was also blocked.

Thus, enhancing the basal $[Ca^{2+}]_{post}$ by increasing the number of postsynaptic bAPs prior to synaptic activation is paralleled by an increased probability for LTP induction. VGCCs (L-type more specifically) play a critical role in this process, as their blockade prevents the rescue of LTP induction by the bAP train. We suggest that LTP induction at L2/3 P–P unitary synaptic connections depends on the interplay between the basal $[Ca^{2+}]_{post}$ preceding synaptic stimulation and the level and dynamics of $[Ca^{2+}]_{post}$ at dendritic spines during synaptic activity.

Effect of Presynaptic Stimuli Occurring during the Postsynaptic bAP Train

A progressive increase in the number of APs in the postsynaptic train increases the probability for LTP induction and induces a switch in the STDP rules. However, if the presynaptic stimulation occurs during, rather than at the very end of the train, multiple bAPs will occur after the presynaptic stimulus. This may result in 1) the induction of LTP, irrespective of whether the presynaptic stimulus occurred before or after the nearest postsynaptic bAP, 2) increased LTP due to a higher Ca^{2+} influx caused by additional bAPs arriving during NMDAR activation (in the 50 Hz train, the additional bAPs will arrive close to the peak of the NMDAR current, should substantially enhance spine Ca^{2+} influx, and therefore might be expected to increase the amount of LTP), or 3) no additional effect on synaptic plasticity. To test this we used the 50 Hz, 10AP postsynaptic train stimulation protocol, but induced synaptic stimulation in the vicinity of the eighth AP ($-5 < \Delta t < 5$ ms) instead. When compared with the standard train-protocol, 3 bAPs, rather than one, now followed the synaptic activation. However, the change in synaptic gain following this stimulation protocol was the same as synaptic stimulation in the vicinity of the 10th AP (Fig. 5*F*). Therefore, the switch in STDP rules occurs even if the presynaptic stimulus arrives during, and not just at the end of, the period of postsynaptic activity.

The Expression Sites of LTP and LTD in L2/3 Pyramidal Cells

To assess the expression site of LTP we measured the PPR in cell pairs in which more than 10% potentiation was obtained. The PPR was significantly reduced after LTP induction in all connections measured (Fig. 6*A*/*a*): 1.1 ± 0.04 in control, compared with 0.87 ± 0.05 ($n = 26$, $p < 0.01$) postconditioning, indicating a presynaptic locus of expression. This suggestion was supported by CV analysis (Fig. 6*A*/*b*), in which a distribution characteristic for entirely presynaptic effects was observed. Strong dependence of LTP on the postsynaptic Ca^{2+} concentration and the presynaptic site of its expression suggest that a retrograde messenger is required for LTP initiation at L2/3 P–P cell synapses.

To test whether the target of a retrograde messenger is the CB_1R, we applied the train-LTP protocol in the presence of AM251, a CB_1R inverse agonist (2 μM; Fig. 6*C*). In all experiments, LTP was induced (1.73 ± 0.24 of control, $n = 4$) indicating that CB_1Rs are likely not involved in LTP induction. We did not address the identity of a retrograde messenger or other probable cannabinoid receptors any further in the present study.

To assess the expression site of LTD we measured the PPR in cell pairs displaying more than 10% synaptic depression ($n = 41$). PPR was 0.95 ± 0.04 in control, and 0.95 ± 0.05 following the conditioning train (Fig. 6*B*/*a*). This indicates a postsynaptic locus of LTD expression, and CV analysis confirmed that, in contrast to L5 pyramidal cells unitary connections and those from L4 spiny stellate to L2/3 pyramids (Sjöström et al. 2004; Bender et al. 2006), synaptic depression is expressed postsynaptically (Fig. 6*B*/*b*). Moreover, AM251 did not inhibit LTD at L2/3 P–P unitary connections (0.73 ± 0.07 of control, $n = 7$; Fig. 6*C*). Meanwhile, in L5 pyramidal cell pairs, AM251 prevented LTD induction (1.07 ± 0.08 of control, $n = 3$) using a standard LTD conditioning protocol (trains of 5 presynaptic and 5 postsynaptic APs; 10 Hz; $\Delta t = -10$ ms) previously utilized by Sjöström et al. (2003).

LTP Depends on NMDAR Activation, whereas LTD Requires Activation of mGluRs

Application of the NMDAR antagonist APV (50 μM) not only inhibited LTP (train-LTP protocol) but actually induced LTD instead (0.7 ± 0.07 of control, $n = 4$; Fig. 6*D*). Meanwhile, LTD induction (train-LTD protocol) was unaffected by APV application (0.73 ± 0.08 of control, $n = 7$; Fig. 6*D*).

Because LTD was NMDAR independent and could not be induced by merely postsynaptic bAPs, we hypothesized that mGluRs might be involved. Indeed, the stimulation protocol (train-LTD protocol) which reliably induced LTD in control conditions (see Fig. 4) did not evoke synaptic depression during coapplication of the group 1 and 2 mGluRs antagonists, CPCCOEt (25 μM) and EGLU (50 μM), respectively. Synaptic

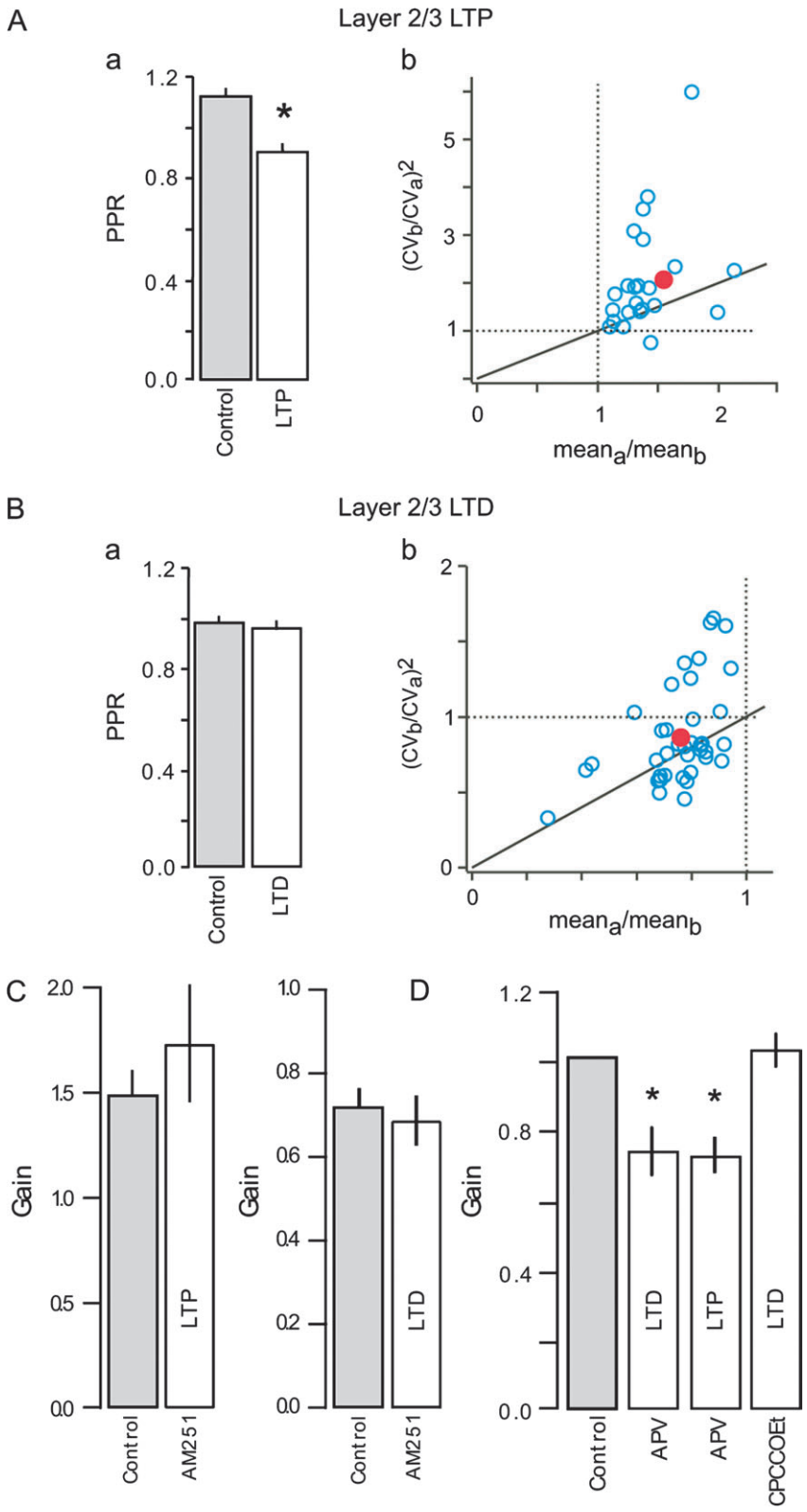

Figure 6. Loci of expression and receptor dependence of STDP in L2/3 P–P connections. (*A*) LTP is expressed presynaptically as demonstrated by (*a*) a significant decrease in PPR after induction of potentiation (*b*) CV analysis ($n = 26$). (*B*) Meanwhile, LTD is expressed postsynaptically as indicated by (*a*) the unchanged PPR after depression induction and (*b*) CV analysis ($n = 26$). (*C*) Both LTP and LTD are unaffected by application of CB1 receptor antagonist (2 μM AM251, $n = 4$ for LTP and $n = 7$ for LTD). (*D*) LTP requires NMDAR activation, whereas LTD is mGluR dependent: 1) LTD ($n = 7$) was not blocked in the presence of 50 μM APV, whereas LTP protocol ($n = 4$) induced LTD in the presence of 50 μM APV; 2) mGluR antagonists prevent LTD induction ($n = 4$). In (*D*), EPSPs were normalized to the mean baseline EPSP amplitude. In all experiments, train-protocols were used for plasticity induction.

gain was 1.02 ± 0.05 of control ($n = 4$, Fig. 6*D*). It was however possible to induce LTP in the presence of mGluR antagonists (1.23 ± 0.12 of control, $n = 4$, data not shown). These results demonstrate that mGluRs play a critical role in the induction of LTD at L2/3 pyramidal cell unitary connections.

Discussion

At L2/3 P–P synapses, the rule of STDP can be converted from one mode (symmetric anti-Hebbian) to another (asymmetric Hebbian) depending on the postsynaptic activity that takes place prior to synaptic activation. Thus, the history of the postsynaptic cell firing shortly before the synaptic input determines which STDP plasticity rule will govern the strength of the unitary connection. This activity-dependent switch depends on the interplay between the basal $[Ca^{2+}]_{post}$ preceding synaptic stimulation and the level and dynamics of Ca2+ at dendritic spines during synaptic activity. LTP induction at these connections is NMDAR dependent and presynaptically expressed, whereas LTD is mGluR dependent and postsynaptically expressed. These data suggest a novel mechanism for regulating which synaptic plasticity rule governs plasticity induction at L2/3 pyramidal cell unitary connections and highlight differences in synaptic plasticity at excitatory synaptic inputs onto L2/3 pyramidal cells.

Location of L2/3 P–P Synapses

Synapse location plays an important role in determining whether bAPs or local signaling is likely to regulate its synaptic plasticity. Differences in STDP time-windows (Froemke et al. 2005), the requirement for NMDAR spikes (Gordon et al. 2006; Kampa et al. 2006) and even a complete inversion of the STDP rule (Letzkus et al. 2006; Sjöström and Häusser 2006) have been observed dependent on whether the synaptic input lies on proximal or distal dendrites. Thus, location-dependent modification of plasticity rules can result in input specificity and play a part in dendritic processing (for reviews see Goldberg et al. 2002; Kampa et al. 2007; Sjöström et al. 2008).

Synapses between L2/3 pyramidal cells are situated mainly on proximal basal dendritic sites (Feldmeyer et al. 2006), at locations which are readily reachable by bAPs in vitro (Köster and Sakmann 1998) and in vivo (Svoboda et al. 1999; Waters et al. 2003). Differences in the exact number and location of synaptic contacts in our study and (Feldmeyer et al. 2006) could be due to differences in interneuronal distances (smaller in our study), and/or differences in local P–P microcircuitry (visual cortex vs. barrel cortex). However, synaptic location does not seem to be a major factor contributing to the "LTD only" induction we observed with low-frequency pre–post pairing.

Simple Spike Timing–Dependent Plasticity Rules at Excitatory Synapses

The simplest STDP protocol consists of single EPSPs paired with single postsynaptic bAPs (Bi and Poo 1998; Froemke and Dan 2002). It has been shown that LTP can be induced by precisely timed pre-before-postsynaptic pairing, whereas post-before-presynaptic pairing can induce LTD, resulting in an asymmetric Hebbian learning rule (Bi and Poo 1998; Froemke and Dan 2002).

At L2/3 P–P synapses however, when neuronal activity is low, a symmetric anti-Hebbian rule governs synaptic plasticity. A similar spike-timing, "LTD only," induction pattern with low neuronal activity has also been observed at CA3-CA1 (Wittenberg and Wang 2006) and L4-L4 spiny stellate synapses (Egger et al. 1999). Indeed, the same single pre-before-single postsynaptic stimulation induces no change (Markram et al. 1997; Pike et al. 1999; Sjöström et al. 2001; Kampa et al. 2006; Nevian and Sakmann 2006), reliable LTP induction (Bi and Poo 1998; Feldman 2000; Froemke and Dan 2002), or the induction of LTD (Tzounopoulos et al. 2004; Zhou et al. 2005; Wittenberg and Wang 2006) dependent on the identity of the synaptic connection. Whether LTP or LTD are induced with single EPSP before single postsynaptic bAP pairing at a particular excitatory synapse will depend on a number of factors including; developmental age (Meredith et al. 2003), dendritic location of the synapses (Letzkus et al. 2006; Sjöström and Häusser 2006), synaptic strength (Bi and Poo 1998), concurrent synaptic inhibition (Meredith et al. 2003), multiple coincidence detectors (Karmarkar and Buonomano 2002; Bender et al. 2006; Nevian and Sakmann 2006), synaptic cooperativity (Sjöström et al. 2001), SK channels (Ngo-Anh et al. 2005), or the width of the bAP (Zhou et al. 2005; Wittenberg and Wang 2006).

Although one simple STDP rule does not "fit all" excitatory synaptic connections, the differences in many, though not all, cases can be explained by differences in levels of postsynaptic depolarization and subsequent Ca2+ influx during the pairing protocol. Indeed, at L5 P–P and CA3-CA1 synapses, synaptic cooperativity (Sjöström et al. 2001) or an increase in the width of the postsynaptic bAP (Wittenberg and Wang 2006), respectively provide the necessary additional conditions for LTP induction.

Given the proximity of L2/3 P–P synaptic connections to the soma it was therefore surprising that additional depolarization or stimulation in Mg^{2+} free extracellular solution (which should cause a dramatic increase in $[Ca^{2+}]_{post}$; Sabatini et al. 2002) did not induce a shift in synaptic gain in our study. The explanations for this could include a low affinity calcium sensor for LTP induction at these contacts and/or insufficient postsynaptic dendritic calcium influx. We therefore increased the amount of postsynaptic activity during the pairing protocol.

bAP Bursts and STDP

Postsynaptic cell bAP burst firing facilitates communication between somatic and distal dendritic sites and can modulate STDP rules (Pike et al. 1999; Meredith et al. 2003; Gordon et al. 2006; Letzkus et al. 2006; Nevian and Sakmann 2006; Sjöström and Häusser 2006; Wittenberg and Wang 2006). It permits LTP induction with single presynaptic stimulation in CA1 pyramidal cells (Pike et al. 1999; Meredith et al. 2003), allows induction of LTP independent of pre–post spike order (Kampa et al. 2006), rescues LTP at distal L2/3 inputs onto L5 pyramidal cells (Letzkus et al. 2006; Sjöström and Häusser 2006) and allows LTP induction at L2/3 proximal (Gordon et al. 2006; Nevian and Sakmann 2006) and distal (Gordon et al. 2006) basal dendrites.

At L5 P–P connections, low-frequency stimulation does not induce a change in synaptic gain, but with a 5 pre- 5-post AP burst protocol (10 Hz or higher) LTP is reliably induced (Markram et al. 1997; Sjöström et al. 2001). Likewise, at L2/3 P–P connections in the barrel cortex, 20 Hz 5 pre- 5 post AP bursts reliably induce LTP (Egger et al. 1999). A low-frequency burst protocol (5 pre- 5 postsynaptic AP burst at 10 Hz) induced LTD at L2/3 visual cortical P–P connections. However

an increase in the burst frequency (pre-before-post) to 20 Hz caused a shift towards LTP, (although this burst frequency was not sufficient to actually induce LTP). This suggests that the relationship between pre–post burst frequency and changes in synaptic gain, whereas similar to that at L2/3 P–P connections in the barrel cortex or L5, is shifted to favor LTD induction with low-frequency pre–post-burst stimulation at L2/3 visual cortical P–P contacts.

Our results suggest that at visual cortex L2/3 P–P connections LTP should be induced with a higher (>20 Hz) 5 pre-5 postsynaptic burst pairing protocol. Alternatively, single EPSPs paired with a high frequency (100–200 Hz) postsynaptic burst protocol could also induce LTP (Gordon et al. 2006; Kampa et al. 2006). However, in this study we focused on the simplest burst paradigm which would retain spike-timing, permit a clear distinction between the contribution of pre- and postsynaptic activity to LTD and LTP induction, and yet provide the requisite postsynaptic depolarization for LTP induction. We therefore used a single presynaptic AP paired with a postsynaptic AP train. We found that a "preconditioning" postsynaptic AP train fundamentally modified the pre–post spike interaction rule and evoked a switch from anti-Hebbian to Hebbian STDP.

Role of Dendritic $[Ca^{2+}]_{post}$ in the Regulation of STDP Rules

The importance of $[Ca^{2+}]_{post}$ elevation in the regulation of STDP has been well documented (for review see Sjöström and Nelson 2002). Burst firing (Pike et al. 1999), Ca^{2+} spikes (Kampa et al. 2006), the distance of synapses from the soma (Froemke et al. 2005; Sjöström and Häusser 2006), and bAP width (Zhou et al. 2005; Wittenberg and Wang 2006) can all regulate the form of STDP rules, by affecting dendritic $[Ca^{2+}]_{post}$ directly during the peristimulus period.

At L2/3 P–P connections we found separate thresholds for LTD and LTP induction. Low-frequency single or burst pairing protocols resulted in "LTD only" induction. Although LTP was NMDAR dependent and was inhibited even by low concentrations of BAPTA, LTD could be induced when NMDARs were blocked and required higher BAPTA concentrations for blockade. Interestingly, an intermediate region where neither LTD nor LTP occurred was also observed with BAPTA application.

A simple peak Ca^{2+} concentration threshold model, however, does not explain the induction of LTD with the preceding 10 AP train, when $[Ca^{2+}]_{post}$ is high, suggesting that additional factors play a role in STDP induction at L2/3 P–P contacts. We found that an additional requirement for the switch in STDP rules is a rise in basal VGCC-dependent $[Ca^{2+}]_{post}$ prior to synaptic stimulation. If VGCCs are blocked or the number of APs in the postsynaptic train is decreased, LTP is no longer induced. The order of these events is however important, as no LTP was induced when the presynaptic stimulus was followed by a postsynaptic 10 AP train.

Finally, spike-timing dependent LTP and LTD could be induced if presynaptic stimulation occurred around the 8th AP or the 10th AP in a 10AP postsynaptic train. Moreover, removing NMDAR's Mg^{2+} block in both train-LTP and train-LTD protocols seemed to abolish the coincidence timing dependence, as LTP was induced in all cases. This suggests that the basal $[Ca^{2+}]_{post}$ preceding synaptic stimulation and the calcium dynamics during synaptic stimulation (with possible supra- or sublinear postsynaptic summation of Ca^{2+} signals (Köster and Sakmann 1998) act in concert to determine the form of the STDP rule at L2/3 P–P connections.

LTP and LTD Induction Mechanisms at L2/3 P–P Connections

Induction of LTP and LTD at L2/3 P–P connections required the activation of 2 different receptor pathways, NMDAR mediated for LTP, and mGluR activated for LTD. Although it is widely accepted that STDP is NMDAR dependent (Magee and Johnston 1997; Bi and Poo 1998; Debanne et al. 1998; Feldman 2000; Sjöström et al. 2001, 2003), an NMDAR-independent component of LTD has also been observed at synapses onto L2/3 pyramidal cells (Feldman 2000; Nevian and Sakmann 2006). mGluR-dependent LTD has also been reported to occur in a wide variety of neurons in different brain regions (Linden et al. 1991; Shigemoto et al. 1994; Hensch and Stryker 1996; Oliet et al. 1997; Egger et al. 1999).

The presence of distinct biochemical signaling cascades for LTP and LTD induction suggest the possibility of 2 separate coincidence detectors for STDP (Karmarkar and Buonomano 2002). This is indeed the case at L4 (Bender et al. 2006) and L2/3 (Nevian and Sakmann 2006) excitatory synaptic connections onto L2/3 pyramidal cells. However, at L2/3 P–P connections a key prediction of the global Ca^{2+}, 2 coincidence detector model, namely that LTD should not be induced at positive Δt intervals with a single EPSP-single postsynaptic AP protocol (Karmarkar and Buonomano 2002), is not met. This suggests that other factors, in this case postsynaptic activity and postsynaptic Ca^{2+} dynamics, play a key part in the induction of bidirectional synaptic plasticity at L2/3 P–P contacts.

LTD is presynaptic and is mediated by retrograde endocannabinoid signaling at L4 (Bender et al. 2006) and L2/3 (Nevian and Sakmann 2006) afferent excitatory inputs onto L2/3 pyramidal cells and at L5 P–P synaptic connections (Sjöström et al. 2003). In contrast, LTD is postsynaptic, and LTP displays a presynaptic expression locus at L2/3 P–P connections. Neither LTD nor LTP are CB_1R dependent, although the postsynaptic VGCC dependence together with the presynaptic expression locus indicate that LTP is mediated by release of a retrograde messenger at L2/3 P–P connections. The differences in LTP and LTD expression loci and signaling pathways at excitatory contacts onto L2/3 pyramidal cells could reflect fundamental differences in properties of excitatory synapses originating in different cortical layers (L2/3-L2/3 vs. L4-L2/3; Brasier and Feldman 2008) or regions (visual cortex vs. barrel cortex). Additionally, they may reflect differences in presynaptic stimulation methods (unitary connections vs. extracellular stimulation) with the possible activation of excitatory afferents whose origins lie outside the local network in the latter case.

Differences in expression locus, retrograde signaling pathways, and calcium dependence at different excitatory synapses onto L2/3 suggest that single L2/3 pyramidal neurons are able to distinguish input sources and use different learning rules based on the origin of input. This input-specific tuning of synaptic gain should greatly enhance the computational capabilities of each individual pyramidal cell within the local neuronal network.

Functional Implications

"Preconditioning" with a postsynaptic spike train can evoke a switch in STDP rule from symmetric anti-Hebbian rule to asymmetric Hebbian. Dependent on the activity of the network, pyramidal cells can therefore determine not only whether LTP or LTD will be induced at a particular synapse, but also which learning rule will govern that change. For this rule switch to be physiologically relevant, L2/3 pyramidal cells should display periods of sparse activity (where the governing rule would be symmetric anti-Hebbian) as well as periods of increased activity (with asymmetric Hebbian rule in effect).

Pyramidal cells in vivo show a range of firing rates in response to sensory stimuli; from low firing rates (<1 Hz) in which "sparse coding" is used to encode information (reviewed in Olshausen and Field 2004), to higher rates 3–>100 Hz (Parnavelas 1984; Softky and Koch 1993; Holt et al. 1996; Shadlen and Newsome 1998; Steriade 2001). Therefore, the required conditions for the rule switch to occur appear to be fulfilled in vivo.

Dynamic functional columns have been suggested to be a means of improving information processing and storage in the cerebral cortex (Diamond et al. 2003). The capability of pyramidal cells to switch between STDP rules suggests a possible mechanism for their formation. Thalamic input is relayed to L2/3 via excitatory afferents from L4 as well as from thalamus itself (Bruno and Sakmann 2006). Input from L4 is reliable and diffuse, and provides an effective lateral spread of excitation for a local population of neurons in L2/3 (Feldmeyer et al. 2002; Shepherd and Svoboda 2005). Following thalamic input, for example, during processing of a sensory task, local pyramidal cells enter an active state, firing trains of APs. LTP at pyramidal cell synapses then becomes possible, allowing the formation of a functional local network by potentiating certain connections and depressing others, according to their relative discharge patterns. In the absence of the thalamic input, pyramidal cells enter a period of sparse activity and LTD is the dominant plasticity outcome. This ability to control the input gain of a limited number of synapses, allows the signal-to-noise ratio of the network to be increased.

Recent studies have shown that the cortex is a dynamic entity; previously potentiated synapses can be "de-potentiated" (weakened), depressed ones can be "de-depressed" (restored or repotentiated) and existing connections constantly form and dissolve over a period of hours (Turrigiano and Nelson 2004; Le Be and Markram 2006). Our results suggest a new way in which "wandering," task-specific functional columns might transiently take shape in the neocortex.

Supplementary Material

Supplementary material can be found at: http://www.cercor.oxfordjournals.org/

Funding

Swedish Medical Research Council funded T.H., Y.Z.; European Molecular Biology Organization Young Investigator Programme funded T.H.; European Commission (HEALTH-F2-2007-201159) to T.H., Y.Z.; National Institutes of Health (DA023214) to T.H.; and the Alzheimer's Association funded T.H.

Notes

We thank M. Häusser, P. J. Sjöström, and G. Stuart for their critical comments on an earlier version of this manuscript. The permanently charged and membrane impermeant verapamil analogue D890 was provided by Abbott Laboratories, Inc. (Abbott Park, IL). *Conflict of Interest*: None declared.

Address correspondence to Dr Yuri Zilberter, Institut de Neurobiologie de la Méditerranée (INMED), Inserm U29, Parc Scientifique de Luminy, 13273 Marseille Cedex 09, France. Email: zilberter@inmed.univ-mrs.fr.

References

Aizenman CD, Manis PB, Linden DJ. 1998. Polarity of long-term synaptic gain change is related to postsynaptic spike firing at a cerebellar inhibitory synapse. Neuron. 21:827–835.

Bender VA, Bender KJ, Brasier DJ, Feldman DE. 2006. Two coincidence detectors for spike timing-dependent plasticity in somatosensory cortex. J Neurosci. 26:4166–4177.

Bi G-Q, Poo M-M. 1998. Synaptic modifications in cultured hippocampal neurons: dependence on spike timing, synaptic strength, and postsynaptic cell type. J Neurosci. 18:10464–10472.

Bi G-Q, Poo M-M. 2001. Synaptic modification by correlated activity: Hebb's postulate revisited. Annu Rev Neurosci. 24:139–166.

Brasier DJ, Feldman DE. 2008. Synapse-specific expression of functional presynaptic NMDA receptors in rat somatosensory cortex. J Neurosci. 28:2199–2211.

Bruno RM, Sakmann B. 2006. Cortex is driven by weak but synchronously active thalamocortical synapses. Science. 312:1622–1627.

Celikel T, Szostak VA, Feldman DE. 2004. Modulation of spike timing by sensory deprivation during induction of cortical map plasticity. Nat Neurosci. 7:534–541.

Conti R, Lisman J. 2002. A large sustained Ca^{2+} elevation occurs in unstimulated spines during the LTP pairing protocol but does not change synaptic strength. Hippocampus. 12:667–679.

Debanne D, Gähwiler BH, Thompson SM. 1998. Long-term synaptic plasticity between pairs of individual CA3 pyramidal cells in rat hippocampal slice cultures. J Physiol. 507:237–247.

Diamond ME, Petersen RS, Panzeri S. 2003. Investigations into the organization of information in sensory cortex. J Physiol (Paris). 97:529–536.

Egger V, Feldmeyer D, Sakmann B. 1999. Coincidence detection and changes of synaptic efficacy in spiny stellate neurons in rat barrel cortex. Nat Neurosci. 2:1098–1105.

Feldman DE. 2000. Timing-based LTP and LTD at vertical inputs to layer II/III pyramidal cells in rat barrel cortex. Neuron. 27:45–56.

Feldmeyer D, Lubke J, Sakmann B. 2006. Efficacy and connectivity of intracolumnar pairs of layer 2/3 pyramidal cells in the barrel cortex of juvenile rats. J Physiol. 575:583–602.

Feldmeyer D, Lubke J, Silver RA, Sakmann B. 2002. Synaptic connections between layer 4 spiny neurone-layer 2/3 pyramidal cell pairs in juvenile rat barrel cortex: physiology and anatomy of interlaminar signalling within a cortical column. J Physiol. 538:803–822.

Froemke RC, Dan Y. 2002. Spike-timing-dependent synaptic modification induced by natural spike trains. Nature. 416:433–438.

Froemke RC, Poo M-M, Dan Y. 2005. Spike-timing-dependent synaptic plasticity depends on dendritic location. Nature. 434:221–225.

Goldberg JK, Holthoff K, Yuste R. 2002. A problem with Hebb and local spikes. Trends Neurosci. 25:433–435.

Golding NL, Staff NP, Spruston N. 2002. Dendritic spikes as a mechanism for cooperative long-term potentiation. Nature. 418:326–331.

Gordon U, Polsky A, Schiller J. 2006. Plasticity compartments in basal dendrites of neocortical pyramidal neurons. J Neurosci. 26:12717–12726.

Harkany T, Holmgren C, Härtig W, Qureshi T, Chaudhry FA, Storm-Mathisen J, Dobszay MB, Berghuis P, Schulte G, Fremeau RT, Jr, et al. 2004. Endocannabinoid-independent retrograde signaling at inhibitory synapses in layer 2/3 of neocortex: involvement of vesicular glutamate transporter 3. J Neurosci. 24:4978–4988.

Hensch TK, Stryker MP. 1996. Ocular dominance plasticity under metabotropic glutamate receptor blockade. Science. 272:554–557.

Holmgren C, Harkany T, Svennenfors B, Zilberter Y. 2003. Pyramidal cell communication within local networks in layer 2/3 of rat neocortex. J Physiol. 551:139–153.
Holt GR, Softky WR, Koch C, Douglas RJ. 1996. Comparison of discharge variability in vitro and in vivo in cat visual cortex neurons. J Neurophysiol. 75:1806–1814.
Kampa BM, Letzkus JJ, Stuart G. 2006. Requirement of dendritic calcium spikes for induction of spike-timing-dependent synaptic plasticity. J Physiol. 574:283–290.
Kampa BM, Letzkus JJ, Stuart GJ. 2007. Dendritic mechanisms controlling spike-timing-dependent synaptic plasticity. Trends Neurosci. 30:456–463.
Karmarkar UR, Buonomano DV. 2002. A model of spike-timing dependent plasticity: one or two coincidence detectors? J Neurophysiol. 88:507–513.
Köster HJ, Sakmann B. 1998. Calcium dynamics in single spines during coincident pre- and postsynaptic activity depend on relative timing of back-propagating action potentials and subthreshold excitatory postsynaptic potentials. Proc Natl Acad Sci USA. 95:9596–9601.
Lambert MP, Barlow AK, Chromy BA, Edwards C, Freed R, Liosatos M, Morgan TE, Rozovsky I, Trommer B, Viola KL, et al. 1998. Diffusible, nonfibrillar ligands derived from Aβ1–42 are potent central nervous system neurotoxins. Proc Natl Acad Sci USA. 95:6448–6453.
Le Be JV, Markram H. 2006. Spontaneous and evoked synaptic rewiring in the neonatal neocortex. Proc Natl Acad Sci USA. 103: 13214–13219.
Letzkus JJ, Kampa BM, Stuart GJ. 2006. Learning rules for spike timing-dependent plasticity depend on dendritic synapse location. J Neurosci. 26:10420–10429.
Linden DJ, Dickinson MH, Smeyne M, Connor JA. 1991. A long-term depression of AMPA currents in cultured cerebellar Purkinje neurons. Neuron. 7:81–89.
Lisman J, Spruston N. 2005. Postsynaptic depolarization requirements for LTP and LTD: a critique of spike timing dependent plasticity. Nat Neurosci. 8:839–841.
Magee JC, Johnston D. 1997. A synaptically controlled, associative signal for Hebbian plasticity in hippocampal neurons. Science. 275: 209–213.
Markram H, Lübke J, Frotscher M, Sakmann B. 1997. Regulation of synaptic efficacy by coincidence of postsynaptic APs and EPSPs. Science. 275:213–215.
Mehta MR. 2004. Cooperative LTP can map memory sequences on dendritic branches. Trends Neurosci. 27:69–72.
Mehta MR, Barnes CA, McNaughton BL. 1997. Experience-dependent, asymmetric expansion of hippocampal place fields. Proc Natl Acad Sci USA. 94:8918–8921.
Meredith RM, Floyer-Lea AM, Paulsen O. 2003. Maturation of long-term potentiation induction rules in rodent hippocampus: role of GABAergic inhibition. J Neurosci. 23:11142–11146.
Nevian T, Sakmann B. 2006. Spine Ca^{2+} signaling in spike-timing-dependent plasticity. J Neurosci. 26:11001–11013.
Ngo-Anh TJ, Bloodgood BL, Lin M, Sabatini BL, Maylie J, Adelman JP. 2005. SK channels and NMDA receptors form a Ca^{2+}-mediated feedback loop in dendritic spines. Nat Neurosci. 8:642–649.
Oliet SHR, Malenka RC, Nicoll RA. 1997. Two distinct forms of long-term depression coexist in CA1 hippocampal pyramidal cells. Neuron. 18:969–982.
Olshausen BA, Field DJ. 2004. Sparse coding of sensory inputs. Curr Opin Neurobiol. 14:481–487.
Parnavelas JG. 1984. Physiological properties of identified cortical neurons. In: Peters A, Jones EG, editors. Cerebral cortex. New York: Plenum Press. p. 205–239.
Pike FG, Meredith RM, Olding AW, Paulsen O. 1999. Rapid report: postsynaptic bursting is essential for 'Hebbian' induction of associative long-term potentiation at excitatory synapses in rat hippocampus. J Physiol. 518:571–576.
Roberts PD, Bell CC. 2002. Spike timing dependent synaptic plasticity in biological systems. Biol Cybern. 87:392–403.
Rubin JE, Gerkin RC, Bi GQ, Chow CC. 2005. Calcium time course as a signal for spike-timing dependent plasticity. J Neurophysiol. 93:2600–2613.
Sabatini BL, Oertner TG, Svoboda K. 2002. The life cycle of Ca^{2+} ions in dendritic spines. Neuron. 33:439–452.
Shadlen MN, Newsome WT. 1998. The variable discharge of cortical neurons: implications for connectivity, computation, and information coding. J Neurosci. 18:3870–3896.
Shepherd GMG, Svoboda K. 2005. Laminar and columnar organization of ascending excitatory projections to layer 2/3 pyramidal neurons in rat barrel cortex. J Neurosci. 25:5670–5679.
Shigemoto R, Abe T, Nomura S, Nakanishi S, Hirano T. 1994. Antibodies inactivating mGluR1 metabotropic glutamate receptor block long-term depression in cultured Purkinje cells. Neuron. 12:1245–1255.
Sjöström PJ, Häusser M. 2006. A cooperative switch determines the sign of synaptic plasticity in distal dendrites of neocortical pyramidal neurons. Neuron. 51:227–238.
Sjöström PJ, Nelson SB. 2002. Spike timing, calcium signals and synaptic plasticity. Curr Opin Neurobiol. 12:305–314.
Sjöström PJ, Rancz EA, Roth A, Häusser M. 2008. Dendritic excitability and synaptic plasticity. Physiol Rev. 88:769–840.
Sjöström PJ, Turrigiano GG, Nelson SB. 2001. Rate, timing, and cooperativity jointly determine cortical synaptic plasticity. Neuron. 32:1149–1164.
Sjöström PJ, Turrigiano GG, Nelson SB. 2003. Neocortical LTD via coincident activation of presynaptic NMDA and cannabinoid receptors. Neuron. 39:641–654.
Sjöström PJ, Turrigiano GG, Nelson SB. 2004. Endocannabinoid-dependent neocortical layer-5 LTD in the absence of postsynaptic spiking. J Neurophysiol. 43:3338–3343.
Softky WR, Koch C. 1993. The highly irregular firing of cortical cells is inconsistent with temporal integration of random EPSPs. J Neurosci. 13:334–350.
Steriade M. 2001. Impact of network activity on neuronal properties in corticothalamic systems. J Neurophysiol. 86:1–39.
Svoboda K, Helmchen F, Denk W, Tank DW. 1999. Spread of dendritic excitation in layer 2/3 pyramidal neurons in rat barrel cortex in *vivo*. Nat Neurosci. 2:65–73.
Turrigiano GG, Nelson SB. 2004. Homeostatic plasticity in the developing nervous system. Nat Rev Neurosci. 5:97–107.
Tzounopoulos T, Kim Y, Oertel D, Trussell LO. 2004. Cell-specific, spike timing-dependent plasticities in the dorsal cochlear nucleus. Nat Neurosci. 7:719–725.
Tzounopoulos T, Rubio ME, Keen JE, Trussell LO. 2007. Coactivation of pre- and postsynaptic signaling mechanisms determines cell-specific spike-timing-dependent plasticity. Neuron. 54:291–301.
Waters J, Larkum ME, Sakmann B, Helmchen F. 2003. Supralinear Ca^{2+} influx into dendritic tufts of layer 2/3 neocortical pyramidal neurons *in vitro* and *in vivo*. J Neurosci. 23:8558–8567.
Wittenberg GM, Wang SS. 2006. Malleability of spike-timing-dependent plasticity at the CA3-CA1 synapse. J Neurosci. 26:6610–6617.
Yoshimura Y, Dantzker JLM, Callaway EM. 2005. Excitatory cortical networks form fine-scale functional networks. Nature. 433:868–873.
Zhou Q, Tao HW, Poo M-M. 2003. Reversal and stabilization of synaptic modifications in a developing visual system. Science. 300: 1953–1957.
Zhou YD, Acker CD, Netoff TI, Sen K, White JA. 2005. Increasing Ca^{2+} transients by broadening postsynaptic action potentials enhances timing-dependent synaptic depression. Proc Natl Acad Sci USA. 102:19121–19125.